Structural characterization and porosity analysis in self Alumina-silica thin films

R.J. Westerwaal[a]
C. den Besten[b]
M. Slaman[b]
B. Dam[a]
D.E. Nanu[c]
A.J. Böttger[c]
W.G. Haije[d]

[a]Delft University of Technology, Department of Chemical Engineering, Materials for Energy Conversion and Storage, Julianaweg 136, 2628 BL Delft, The Netherlands
[b]Vrije Universiteit Amsterdam, Department of Physics and Astronomy, De Boelelaan 1081, 1081 HV Amsterdam, The Netherlands
[c]Delft University of Technology, Department of Materials Science and Engineering, Mekelweg 2, 2628 CD Delft, The Netherlands
[d]Energy Research Centre of the Netherlands, Hydrogen Production & CO2 Capture, Westerduinweg 3, 1755 LE Petten, The Netherlands

Published in Elsevier 36 (2011) 1074-1082

ECN-W--11-057

NOVEMBER 2011

Available at www.sciencedirect.com

ScienceDirect

journal homepage: www.elsevier.com/locate/he

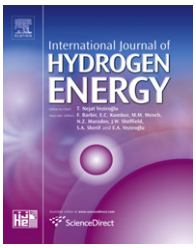

High throughput screening of Pd-alloys for H_2 separation membranes studied by hydrogenography and CVM

R.J. Westerwaal [a,*], C. den Besten [b], M. Slaman [b], B. Dam [a], D.E. Nanu [c], A.J. Böttger [c], W.G. Haije [d]

[a] Delft University of Technology, Department of Chemical Engineering, Materials for Energy Conversion and Storage, Julianaweg 136, 2628 BL Delft, The Netherlands
[b] Department of Physics and Astronomy, Vrije Universiteit Amsterdam, De Boelelaan 1081, 1081 HV Amsterdam, The Netherlands
[c] Department of Materials Science and Engineering, Delft University of Technology, Mekelweg 2, 2628 CD Delft, The Netherlands
[d] Energy research Centre of The Netherlands, Westerduinweg 3, 1755 LE Petten, The Netherlands

ARTICLE INFO

Article history:
Received 3 July 2010
Received in revised form
29 September 2010
Accepted 2 October 2010
Available online 25 October 2010

Keywords:
Pd-alloys
Thermodynamics
Cluster variation method
Hydrogen absorption
Hydrogenography
Critical temperature

ABSTRACT

The search for and development of stable Pd-based membranes for hydrogen separation applications with resistance to hydrogen embrittlement and cracking is a challenging and time-consuming task. Membrane failure is most often caused by the occurrence of the $\alpha-\beta$ phase transition during hydrogen absorption and desorption by the Pd-alloy below the critical temperature. By finding a suitable alloy with a critical temperature below room temperature, the membrane lifetime can be extended tremendously. Here we present a combinatorial approach that enables the fast screening of phase transitions in multi-component Pd-alloys for hydrogen separation membranes by experiments and thermodynamic calculations. The method is applied to the well-documented Pd–Cu alloy compositions. Hydrogenography, a compositional gradient thin film technique, is used to experimentally investigate the alloy compositions. Using a new phenomenological method to determine the critical temperature from hydrogenography measurements, we show that the experimental results and the calculations, using the Cluster Variation Method (CVM), agree well with the phase boundaries and critical temperatures reported in literature. Our results show that the combined capabilities of hydrogenography and CVM enable an efficient screening of promising multi-component alloys for which thermodynamic data are scarce or absent.

1. Introduction

The use of membrane reactors equipped with Pd-based membranes is a promising technology to separate high-purity hydrogen from natural gas and coal gasification gas streams [1,2]. A major challenge is the development of Pd-based alloys, which are stable during long-term use and numerous hydrogenation cycles. Besides being able to operate at high temperatures (>625 K) and pressures (40 bar), these membranes need to have a high hydrogen permeability [3,4] and high resistance towards poisoning effects by contaminants like H_2S, C, CO, CO_2 [5]. However, the mechanical, chemical and thermal stability are equally important [6–8].

Membrane failure is mostly related to hydrogen embrittlement and cracking of the active Pd-based membrane layer caused by the $\alpha-\beta$ phase transition at temperatures below the

* Corresponding author.
E-mail address: ruudwesterwaal@hetnet.nl (R.J. Westerwaal).
0360-3199/$ – see front matter © 2010 Professor T. Nejat Veziroglu. Published by Elsevier Ltd. All rights reserved.
doi:10.1016/j.ijhydene.2010.10.014

critical temperature [9–11]. This phase transition occurs mainly during start up and shut down of the membrane reactor and for pure Pd this is accompanied by a considerable volume expansion of $\Delta V_{\beta-\alpha}/V\alpha = 10\%$. Furthermore, due to the clamping of the membrane to the carrier substrate, hysteretic effects associated to the hydrogen induced expansion of the membrane with respect to the carrier, cannot be excluded [12]. These effects indicate that the stability and lifetime of Pd-based membranes can be improved considerably by suppressing the α–β phase transition, hence, by reducing the critical temperature (T_c) below room temperature.

A possible way to lower the critical temperature is by e.g. alloying the Pd, but given the amount of alloying elements and compositions which need to be screened this is not a trivial task. For Pd–Cu and Pd–Ag alloys it is known that the T_c decreases as function of increasing Cu and Ag concentration [13,14]. Furthermore, these alloys have the additional advantage of being more resistant towards contaminations [5,15–17] and having a sufficient or even improved permeability as compared to pure Pd [3–5,18–20] while the reduction of the amount of Pd results also in a cost benefit [21,22]. However, it is found that the critical temperature is not uniquely determined as it is influenced by properties like crystallinity, grain size, stress development, interaction with the carrier substrate etc. For pure bulk Pd the T_c ranges from 556 K [23] to 566 K [24], while for Pd films T_c's of 528 K [25], 542 K (50 nm thin film), and 568 K (300 nm thin film) are found [26,27]. This indicates that the characterization of kinetic and thermodynamic properties, especially the determination of the critical temperature, is not a trivial task and becomes even more challenging for alloys. For an accurate determination of the critical temperature, the alloy phase should be well-defined. This is often difficult to realize in practice due to incomplete alloy formation, phase segregation and stress effects.

The practical necessity to find reliable Pd-based membranes capable to operate under harsh conditions, leads to a strong need for the development of accurate high throughput characterization techniques. The thin film combinatorial screening technique called hydrogenography has so far been applied successfully in the development of hydrogen sensors [28,29] and materials for hydrogen storage [30,31]. Here we show its applicability to determine the critical temperature of promising multi-component Pd-alloys for hydrogen separation membranes. In addition, we combine the thin film hydrogenography technique with the cluster variation method (thermodynamic CVM calculations) based on input of data from binary (bulk) alloys [14]. This coupled approach enables us to identify candidate alloys and examine their hydrogenation properties around the critical point. Our focus here is on the development of a new method which we apply to the rather well-documented Pd–Cu system.

2. Methodology

In the following we will give a detailed description of the experimental and theoretical techniques and show how their combination can yield reliable and accurate quantitative information about the alloy properties in a fast and efficient way, especially around the critical point.

2.1. *Hydrogenography*

Generally, Sieverts-type measurements are used to determine the sorption characteristics of metal alloys. However these methods are extremely time-consuming. Therefore, they are not very well suited for a fast characterization of the hydrogenation properties of a large number of alloys. As a consequence, the systematic characterization of multi-component alloys is rare and often limited to a narrow range of alloy compositions.

Hydrogenography differs from Sieverts'-type measurements as it is a high throughput experimental thin film technique. The technique is based on the property that hydrogen absorption by a thin metal film results in optical changes of the film. Using a simple optical transmission setup, a hydrogen loading cell (pressure up to 10 bar) and an oven (temperature ranging from 305 K to 573 K), properties such as the plateau pressure and critical temperature are determined quantitatively. By using a thin film with a compositional gradient, it is possible to investigate the thermodynamic and kinetic hydrogenation properties of continuous series of alloy compositions simultaneously under the same experimental conditions [31,32].

Pd–Cu gradient thin films with a thickness from 50 to 80 nm (depending on composition) are deposited at room temperature on glass substrates in an ultrahigh-vacuum dc magnetron co-sputtering system (base pressure 10^{-9} mbar, deposition pressure 0.003 mbar). Pd-rich gradient thin films (up to 30 at.% Cu) are investigated thus avoiding any bcc–fcc phase transitions [33,34]. To reduce strain effects due to clamping of the film by the glass substrate, a 3 nm thick Pd intermediate layer is deposited between the Pd-alloy gradient film and substrate ((Pd)Pd–Cu). This allows us to study the hydrogenation behavior of quasi-free thin films [12].

To determine the film thickness and Pd–Cu composition at all (gradient) positions, tooling samples have been used. The thickness of pure Pd and Cu thin films is measured with a DEKTAK profilometer, from which the thickness profile of the Pd–Cu alloy is determined. Subsequently the position dependent composition is calculated by using the atomic volumes of Pd and Cu. Furthermore, the ratio of the elements in the gradient sample is verified by Rutherford Back Scattering Spectrometry, resulting in a compositional map of the sample. At different sample positions the Cu and Pd concentrations are determined and compared with the results obtained with the DEKTAK profilometer. The results are consistent and a fitting procedure gives a relation between the position on the sample and composition.

Upon hydrogenation, we relate the concentration of the β (hydride) phase to the optical transmission by the Lambert–Beer relation, assuming that the α and β phases are properly mixed. In the two-phase region, the sum of the fractions of the system that is either in the α or in the β phase is normalized to 1, that is $x_\alpha + x_\beta = 1$, with x_α and x_β the fractions of the α and β phases. Assuming a homogeneous distribution of the phases, the intensity of the light reaching the CCD camera is given by,

$$I(x_\alpha, x_\beta) = I_0 \times e^{\left(-\mu_\alpha x_\alpha - \mu_\beta x_\beta\right)t} + I_B \quad (1)$$

with I the intensity of the transmitted light, I_0 the initial light intensity before reaching the sample, I_B the background light intensity detected by the CCD camera, μ_α the absorption coefficient at the maximum hydrogen concentration (α_{max}) of the α-phase, μ_β the absorption coefficient at the minimum hydrogen concentration (β_{min}) of the β-phase, and t the local thickness of the film. Then the transmission of the sample is defined as,

$$T \equiv I(x_\alpha, x_\beta) - I_B = I_0 \times e^{\left(-\mu_\alpha x_\alpha - \mu_\beta x_\beta\right)t} \quad (2)$$

Before hydrogen absorption the initial transmission T_0 is given by,

$$T_0 \equiv T(x_\alpha = 1, x_\beta = 0) = I_0 \times e^{\left(-\mu_{\alpha,0}\right)t} \quad (3)$$

here $\mu_{\alpha,0}$ the absorption coefficient for the metallic state. Using the relation $x_\alpha + x_\beta = 1$ this results in the following relation stating that in the two-phase region the hydrogen concentration scales linearly with the logarithm of the normalized transmission. Formally, this equation only holds in the two-phase region because outside this region the dependence of the transmission on the hydrogen cencentration differs from the Lambert–Beer relation.

$$\ln\frac{T}{T_0} = (\mu_{\alpha,0} - \mu_\alpha)t + (\mu_\alpha - \mu_\beta)tx_\beta \quad (4)$$

T_0 is the transmission through the film in the as-prepared state and T the optical transmission during hydrogenation. As long as the sample loads uniformly, the Pressure–-Transmission-Isotherms (PTI) give the same equilibrium pressure and are qualitatively analogous to "classical" Pressure Composition Isotherms (PCI) obtained with standard volumetric or gravimetric methods on bulk samples [12]. To obtain an (quasi-)equilibrium state between the applied hydrogen gas and the hydrogen in the Pd–Cu film, the pressure is increased, depending on the set temperature, in small linear or logarithmic pressure steps with after each pressure step a relaxation time. The determination of the critical temperature is not straightforward and we developed three new phenomenological methods for the determination of the critical temperature from hydrogenography measurements, see Fig. 1:

a) Image fit method
b) Phase boundary method
c) Boltzmann fit method

The image fit method determines the critical concentration from a hydrogenography image of a gradient sample. In Fig. 1a we display how the optical transmission (color) of a gradient alloy film changes when slowly increasing and decreasing the hydrogen pressure. Upon increasing the hydrogen pressure, the α–β phase transition occurs up to the critical composition (left part of Fig. 1a) and upon reducing the hydrogen pressure the reverse phase transition occurs (right part of Fig. 1a). Between the α-phase (dark region, low hydrogen concentration) and β-phase (light region, higher hydrogen concentration) a sudden change in transmission occurs. This change in transmission will disappear at the critical Cu concentration since above this concentration only one phase exists. This boundary can be fitted by a second order polynomial. If the temperature is below the critical temperature of any of the alloys probed in the gradient film, a flat top (transmission does not change with pressure as indicated by the horizontal line) will appear between the two branches of the polynomial. At this specific Pd–Cu ratio the polynomial fit fails. The junction between the parabola branches and the flat top determines the critical Cu concentration with a standard deviation of 1.5 at.% Cu.

The phase boundary method determines the critical temperature at a single alloy composition from an extrapolation of the Pressure-Transmission-Isotherms (PTI's), see Fig. 1b. We fit the α_{max} and β_{min} phase boundaries as obtained from the optical transmission measurements ($\ln(T/T_0)$) by a second order polynomial. At the critical temperature the difference between α_{max} and β_{min} disappears, thus the top of the parabola corresponds to the critical temperature.

The Boltzmann method again analyses the PTI's of individual alloy compositions. It is based on a Boltzmann fit through the PTI plateau region with,

$$\ln(T/T_0) = \frac{A_1 - A_2}{1 + \exp\left(\frac{p - p_{PLAT}}{dp}\right)} + A_2 \quad (5)$$

A_1, A_2 and dp are constants depending on the specific measured PTI, p the applied H_2 pressure and p_{PLAT} is the plateau pressure. The plateau pressures are determined by the maximum value of the derivative of the Boltzmann fit. Between the logarithm of the plateau pressures and the corresponding Cu concentrations, a linear relation is found, as was shown already by Flanagan et al. [41], see Fig. 1c. A strong deviation from this linear behavior signifies the presence of the critical concentration. The plateau pressures are determined with steps of 0.5% in Cu concentration.

As we will show, these three methods result in comparable critical temperatures. Note that in all experiments, we cycled the films until we observe a reproducible behavior reflecting the intrinsic nature of the transition.

2.2. *Statistical thermodynamic approach: cluster variation method*

The influence of alloying Pd with Cu on the critical temperature and the α (low hydrogen content) – β (high hydrogen content) phase boundaries is determined by a statistical thermodynamical approach. We calculated the phase boundaries using the cluster variation method (CVM) [35]. The energy functional used in the CVM is expressed in terms of small groups of atoms (clusters) for which correlated occupancies are considered. This model has been put forward recently as a tool to design new Pd-alloys [13,14] and has proven successful in the determination of thermodynamic properties of interstitial systems [36]. Phase equilibria between α and β phases of binary, ternary or multi-component alloys are predicted based on available experimental bulk data of *binary* alloys. The model takes into account the volume changes due to the α–β transition, and the possible order–disorder transitions. For the purpose of modelling, the structure is described as consisting of a fully occupied fcc host metal matrix, with hydrogen occupying the octahedral sites

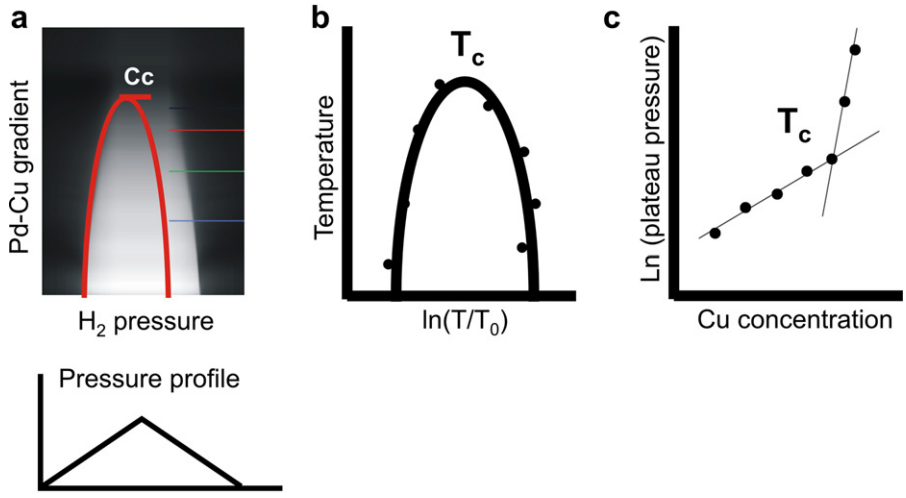

Fig. 1 – Schematic representation of the determination of the critical temperatures with hydrogenography by the 3 proposed methods. a) hydrogenography image fit method, b) phase boundary method, c) Boltzmann fitting method.

only. The sublattice, consisting of the octahedral sites, also forms an fcc structure with its sites occupied by H and/or vacancies. The basic cluster used is a tetrahedron formed on the interstitial fcc sublattice: in this case the interstitials are described in the mean field of the metal host.

This approach implicitly contains the vibrational contributions to the entropy and energy through the use of effective pair interaction parameters based on experimental thermodynamic data (at room temperature). Those data contain all the energy contributions; in the relatively small temperature range considered and T well above the Debye temperature, the temperature dependence of the vibrational contribution is small and is not needed to describe the phase boundaries well. Previous work on interstitial systems [38] showed that when the (much more cumbersome) ab initio calculations approach is used instead of effective pair potentials, the Debye-Gruneisen model can be used to describe the T dependence of the vibrational contributions.

The corresponding critical temperatures are obtained by fitting the concentration differences at the phase boundary i.e. $c(\beta_{min})-c(\alpha_{max})$ as function of temperature using a second order polynomial. The extrapolation to the temperature where $c(\beta_{min}) = c(\alpha_{max})$ is considered as T_c. This is an empirical method i.e. there is not a known linear relation between $c(\beta_{min})-c(\alpha_{max})$ and the temperature, but it can be fitted accurately with a second order polynomial. Additional details about the CVM calculation method are described elsewhere [13,14].

3. Results and discussion

3.1. *Pressure-transmission-isotherms and phase boundaries*

Thin films allow a fast scanning of the physical properties. While the presence of a substrate may influence the hydrogenation properties, we have shown that in Pd the isotherms reproduce those of bulk samples [12]. This implies that also the critical point in thin films are representative for that of bulk samples. To determine the critical point, pressure-transmission-isotherms (PTI) of several Pd–Cu thin films are measured as a function of the Cu concentration. Fig. 2 shows the PTIs at 307 K, 323 K and 353 K as obtained from the optical transmission of a $Pd_{95}Cu_5$ thin film. We find that the plateau pressures closely resemble those found by Sakamoto et al. [37] obtained on 50–100 μm thick foils. The plateaus resulting from the coexistence of the α and β phases show a slope, which is most likely due to strain development in the film during hydrogenation. However, the equilibrium hydrogen pressure (as determined by Boltzmann fitting) is the same as that found for bulk samples [37,39]. The width of the plateaus quickly reduces with increasing temperature, indicating the proximity of the critical temperature at this Cu concentration.

Instead of determining the PTI diagrams for each Cu concentration separately, hydrogenography enables one to measure numerous $Pd_{100-x}Cu_x$ isotherms simultaneously in a gradient thin film sample. Thus, in a single hydrogenation run we obtain the plateau pressures for many $Pd_{100-x}Cu_x$ alloys at a given temperature. In Fig. 3 the hydrogen absorption and desorption cycle of such a Pd–Cu gradient sample with compositions between $Pd_{55}Cu_{45}$ and $Pd_{92}Cu_8$ is shown. Upon increasing the hydrogen pressure slowly from 1 mbar to 1 bar, at low Cu concentrations a well-defined optical change is observed (formation of the transparent β phase). At higher Cu concentrations the pressure needed to obtain an optical transition increases, while it finally becomes fuzzy and disappears altogether on the left side of the picture. Upon decreasing the applied hydrogen pressure, the $Pd_{100-x}Cu_x$–H film returns to its de-hydrogenated state, as is illustrated by the transition to the less-transparent state. As the optical transparency is related to the hydrogen concentration in the film, isotherms can be obtained for any composition of the gradient film. The measured PTIs at 308 K for the compositions $Pd_{85}Cu_{15}$, $Pd_{80}Cu_{20}$, $Pd_{75}Cu_{25}$, and $Pd_{72}Cu_{28}$ (colored lines in Fig. 3) are shown in Fig. 4. Again the correspondence with the bulk data is quite good. In both cases we observe a small

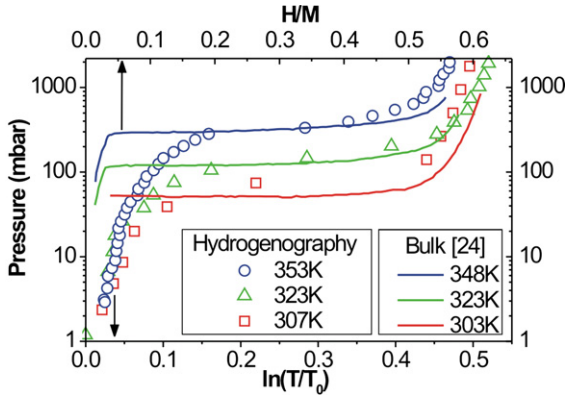

Fig. 2 – Hydrogenography PTI's of a 38 nm $Pd_{95}Cu_5$ thin film. The results of Sakamoto et al. on bulk samples are shown for comparison [37]. The upper horizontal axis indicates the ratio of the number of hydrogen atoms to the total number of metal atoms and the lower horizontal axis shows the hydrogen concentration as $\ln(T/T_0)$ according to hydrogenography.

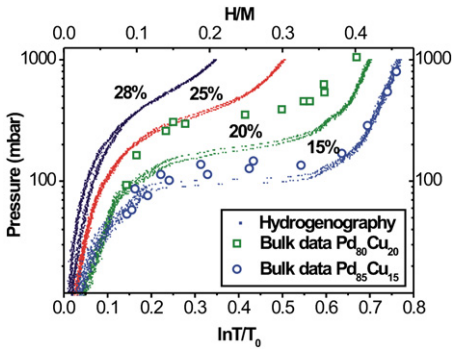

Fig. 4 – PTI's for different Cu concentrations measured at 308 K during hydrogen absorption and desorption. For lower Cu concentrations a hysteresis is observed in both the hydrogenography isotherms as bulk isotherms [39].

hysteresis, which for Pd has been attributed to coherency strain induced by the phase transformation [40]. This hysteresis is expected to vanish above the critical temperature. Indeed, from Fig. 4 we conclude that at 308 K, the hysteresis effect disappears between the compositions $Pd_{80}Cu_{20}$ and $Pd_{72}Cu_{28}$. Furthermore, the plateau pressure and slope increase whereas the coexistence region of the α–β phases appears to decrease with increasing Cu concentration.

The narrowing of the two-phase region for an increasing Cu content at a constant temperature is also found in the corresponding CVM calculations. When compared to the isotherms for pure Pd, the isotherms of $Pd_{100-x}Cu_x$ alloys shift towards higher pressures as function of increasing Cu concentration and therefore the hydrogen capacity in pure Pd is always higher than for any Pd–Cu alloy [39]. I.e. isobaric hydrogen capacity decreases with an increasing Cu fraction [37]. For the Pd–Cu–H system, the phase boundaries calculated by the CVM for the corresponding compositions are shown in Fig. 5. The lines indicate the phase boundaries calculated by the CVM and the marks correspond to (experimental) literature data [37,39,41]. The calculations show that hydrogen solubility (α_{max}) increases while the hydrogen capacity (β_{min}) decreases with increasing Cu concentration. The decrease in the strength of the effective field of the metal sublattice and the relative interaction strength between nearest-neighbor occupied (H) and unoccupied (vacant) interstitial sites with increasing Cu content, reduces the miscibility gap [14]. Furthermore, a very good agreement between the CVM calculated phase boundaries and literature

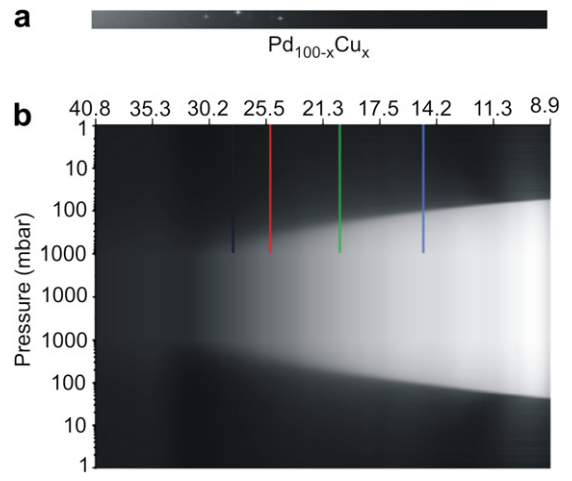

Fig. 3 – Hydrogenography image of the Pd–Cu gradient sample in a) the as-prepared state and b) during a full hydrogenation cycle. Figure a) shows a few film defects (light spots) and on the Cu rich side a higher transmission (I_0). The lines indicate the positions from which we derive the PTI's.

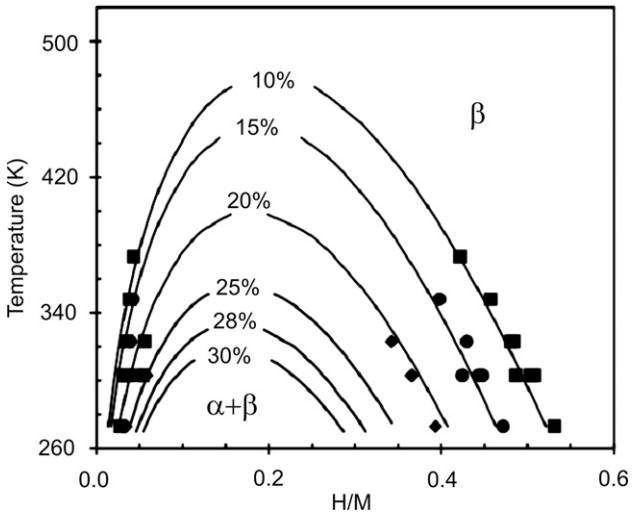

Fig. 5 – Comparison of CVM calculated (solid lines) and (experimental) literature data (symbols) phase boundaries in $Pd_{100-x}Cu_x$–H systems with $x = 10$, 15, 20, 25, 28 and 30 at.% Cu. Symbols in the inset represent experimental data for (■) $Pd_{90}Cu_{10}$–H [37,39], (●) $Pd_{85}Cu_{15}$–H [37,39], and (◆) $Pd_{80}Cu_{20}$–H [37,39] systems.

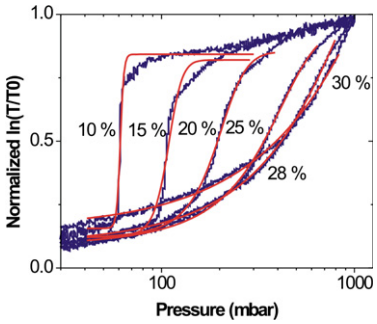

Fig. 6 – Normalized pressure-transmission-isotherms versus pressure and fitted with a Boltzmann function in the plateau region for the Cu concentrations 10, 15, 20, 25, 28 and 30 at.% at 308 K.

data [37,39,41] is found, indicating the predictive abilities of CVM calculations for unknown alloy compositions.

3.2. *Critical temperature determination*

The observed agreement between hydrogenography, CVM calculations and literature data on the obtained plateau pressures, provides a reliable basis for the determination of the critical point. While the three methods to derive the Tc from hydrogenography lead to more or less the same result, we focus in Fig. 6–Fig. 7 on a number of pictures illustrating the Boltzmann method. First, for various concentrations, the isotherms are fitted with a Boltzmann function (Fig. 6), then

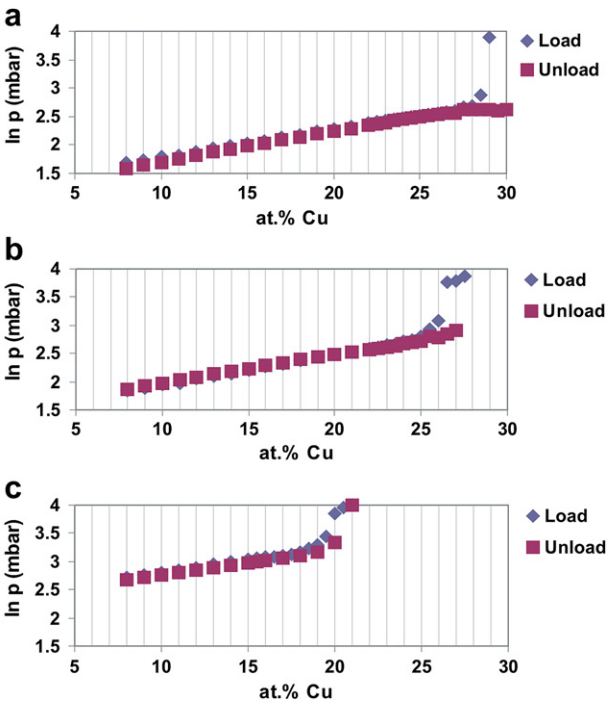

Fig. 7 – Plateau pressure as function of Cu concentration measured at a) 308 K, b) 323 K, and c) 373 K during hydrogen absorption and desorption for a (Pd)Pd–Cu gradient thin film.

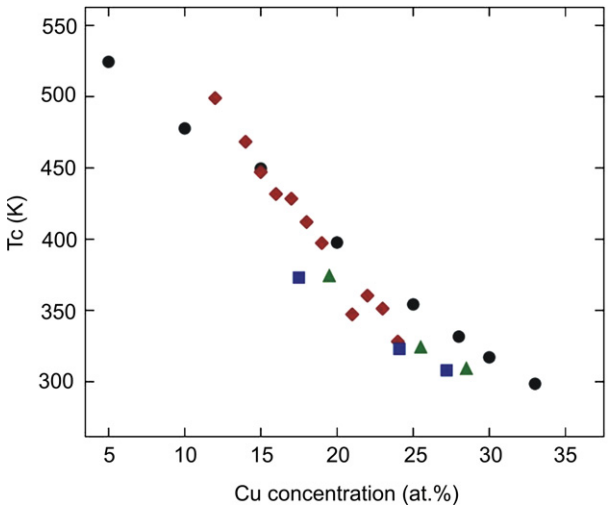

Fig. 8 – Critical temperature for α–β phase transition as function of Cu concentration as determined by CVM calculations (●) and by hydrogenography using the image fit method (■), phase boundary method (◆) and Boltzmann fit method (▲).

the plateau pressure thus obtained is plotted versus the Cu concentration (at various temperatures, see Fig. 7). From the sudden change in slope, a critical point can be determined very well. The critical temperatures as determined by the various hydrogenography methods and the CVM calculations for various Cu concentrations are summarized in Fig. 8. The critical temperatures follow the same trend as function of Cu content. The critical temperature decreases almost linearly with increasing Cu concentration from ~530 K for the composition $Pd_{95}Cu_5$ to ~300 K for $Pd_{67}Cu_{33}$. Comparing the three methods based on hydrogenography we find that at higher Cu concentrations (>15%) the image fit method, phase boundary method and Boltzmann fit method result in lower Tc's as compared to the values found by CVM, whereas at lower Cu concentrations the phase boundary method results in higher

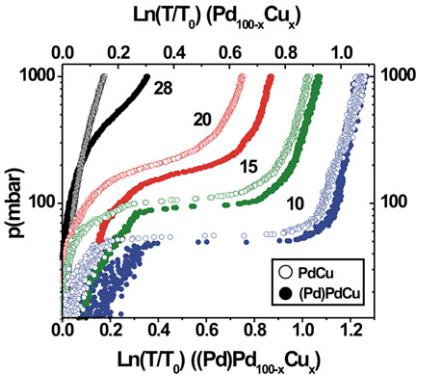

Fig. 9 – Dehydrogenation measurement at 308 K showing the difference between a Pd–Cu gradient film directly deposited on the substrate (Pd–Cu) and with a 3 nm Pd layer between the substrate and the Pd–Cu gradient thin film ((Pd)Pd–Cu).

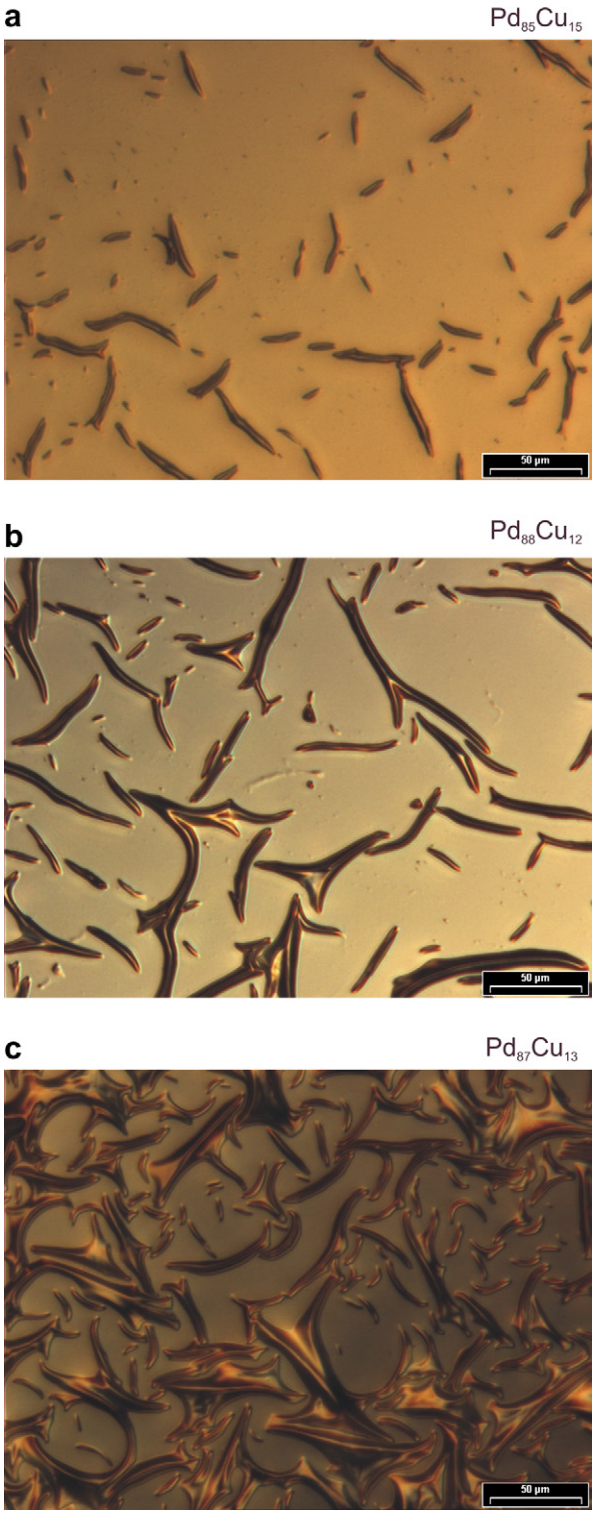

Fig. 10 – Micrographs (in reflection) of Pd–Cu thin films deposited directly on a glass support: a) $Pd_{85}Cu_{15}$ after 7 hydrogenation cycles, b) $Pd_{88}Cu_{12}$ after 7 hydrogenation cycles, c) $Pd_{87}Cu_{13}$ after 15 hydrogenation cycles at room temperature.

Tc's compared to CVM. The image fit and Boltzmann fit method have a comparable slope to the CVM calculations but underestimates the Tc values, where as the phase boundary method has a bit different slope in Tc values. Although, the films are provided with a 3 nm Pd intermediate layer between the Pd–Cu gradient film and substrate, possibly the T_c values in our thin films are still affected by the substrate [12,42].

To that the influence of thin film clamping on the critical temperature is investigated by comparing hydrogenography measurements with and without a 3 nm Pd intermediate layer, see Fig. 9. For the gradient film without a Pd intermediate layer, the plateau pressures shift towards higher pressures and a larger slope is found as compared to films with a Pd intermediate layer. As a consequence a somewhat lower T_c is found for a thin film directly deposited on a glass substrate. Thus a Pd interlayer reduces the stress development in the thin film system which results in a critical temperature close to bulk-values.

The isotherms, critical temperature and hysteresis effect are all influenced by stress effects in the film during hydrogen absorption and desorption [40,43,44]. This strain development has its origin in the coherency strain at the transforming α and β phases (which is also present in bulk samples) [40,43,44] and the coherency strain induced by the sticking of the film on the substrate (elastic boundary conditions) [45]. In thin films, the clamping effect to the substrate will weaken the attractive H–H interaction and as a consequence of a decreased H–H interaction energy, the apparent critical temperature decreases [46].

Since the noble metal Pd forms a less strong bond with the substrate (glass) as compared to Cu, lowering the Cu concentration results in a reduced sticking of the Pd–Cu film to the substrate. To illustrate this effect, reflection micrographs of thin Pd–Cu films are shown in Fig. 10. In Fig. 10a and b the surface of a $Pd_{85}Cu_{15}$ and a $Pd_{88}Cu_{12}$ thin film are shown after 7 hydrogenation cycles. The thin film with a higher Cu concentration ($Pd_{88}Cu_{15}$) shows significally less buckling than the film with a lower Cu concentration, whereas the buckling increases with hydrogenations cycles, see Fig. 10b and c. The Cu acts as a sticking material to the substrate resulting in less buckling and higher plateau pressures. Therefore, the pure Pd intermediate layer allows buckling of the film during hydrogenation, which releases almost all stress. This has the effect of creating a quasi-free standing Pd–Cu gradient film that has a critical temperature which is comparable to bulk-values [46]. For comparison, Fisher et al. indicate that the α and β phase are no longer formed at 298 K and 35 at.% Cu, in good agreement with our results [47].

Furthermore, for future research the combination of hydrogenography and CVM calculations results in a methodology which allows identification of the most promising multi-component Pd-alloys for specific membrane applications. First by CVM calculations the phase boundaries and critical temperature of a not yet synthesized multi-component Pd-alloy containing hydrogen are determined. Based on these results the most promising allows can be selected and be characterized with hydrogenography.

4. Conclusions

Hydrogenography measurements on Pd–Cu alloys show that this technique is a reliable high throughput screening method to develop new Pd-based alloys for hydrogen separation

membranes. We found a reliable method to determine the critical temperature from these measurements. The determination of the critical temperature is essential for the design of a separation membrane which is able to operate at water gas shift conditions in hydrogen production. The experimental results are in agreement with CVM calculations and literature data and this indicates that hydrogenography on thin films gives results that are comparable to conventional bulk methods. The best agreement between bulk and thin film data is obtained when using a Pd interlayer between the film and the substrate thereby creating a quasi-free film.

Hydrogenography in combination with the cluster variation method can thus be used to "design" a Pd-alloy with the desired phase stability in a certain hydrogen concentration-temperature range. The methodology comprises two steps: first the phase boundaries and critical temperature of a not yet synthesized multi-component Pd-alloy containing hydrogen are calculated. Next, based on the calculations, the alloys that show no phase transition in the desired temperature and pressure window are selected. The second step consists of the preparation of thin film specimens by magnetron sputtering and the experimental determination of the actual critical temperatures by hydrogenography.

The method to design and characterize new alloys can easily be extended to multi-component alloys for which thermodynamic data are scarce or absent. The combination of hydrogenography and CVM calculations is therefore a powerful tool for a fast and efficient determination of promising multi-component Pd-alloys for hydrogen separation membranes.

Acknowledgements

The authors are grateful to H. Schreuders for technical support and sample preparation. Part of this work has been financed by the Dutch ministry of economic affairs in the framework of a SenterNovem EOS-LT grant (EOSLT07008) and the authors acknowledge financial support from the Nederlandse Organisatie voor Wetenschappelijk Onderzoek (NWO) through the Sustainable Hydrogen Programme of Advanced Chemical Technologies for Sustainability (ACTS).

REFERENCES

[1] Barelli L, Bidini G, Gallorini F, Servili S. Hydrogen production through sorption-enhanced steam methane reforming and membrane technology: a review. Energy 2008; 33:554–70.
[2] Ockwig NW, Nenoff TM. Membranes for hydrogen separation. Chem Rev 2007;107:4078–110.
[3] Ward TL, Dao T. Model of hydrogen permeation behavior in palladium membranes. J Membr Sci 1999;153:211–31.
[4] Moss TS, Peachey NM, Snow RC, Dye RC. Multilayer metal membranes for hydrogen separation. Int J Hydrogen Energy 1998;23(2):99–106.
[5] Howard BH, Killmeyer RP, Rothenberger KS, Cugini AV, Morreale BD, Enich RM, et al. Hydrogen permeance of palladium–copper alloy membranes over a wide range of temperatures and pressures. J Membr Sci 2004;241(2):207–18.
[6] Paglieri SN, Way JD. Innovations in palladium membrane research. Sep Purif Methods 2002;31(1):1–169.
[7] Yuan L, Goldbach A, Xu H. Permeation hysteresis in PdCu membranes. J Phys Chem B 2008;112:12692–5.
[8] Kulprathipanja A, Alptekin GO, Falconer JL, Wayc JD. Pd and Pd–Cu membranes: inhibition of H_2 permeation by H_2S. J Membr Sci 2005;254:49–62.
[9] Shu J, Bongondo BEW, Grandjean BPA, Kaliaguine S. Morphological changes of Pd–Ag membranes upon hydrogen permeation. J Mater Sci Lett 1997;16:294.
[10] Yan S, Maeda H, Kusakabe K, Morooka S. Thin palladium membrane formed in support Pores by metal-Organic chemical Vapor deposition method and application to hydrogen separation. Ind Eng Chem Res 1994;33:616.
[11] Javarama V, Lin YS. Synthesis and hydrogen permeation properties of ultrathin palladium–silver alloy membranes. J Membr Sci 1995;104:251.
[12] Pivak Y, Gremaud R, Gross K, Gonzalez-Silveira M, Walton A, Book D, et al. Effect of the substrate on the thermodynamic properties of PdHx films studied by hydrogenography. Scr Mater 2009;60(5):348–51.
[13] Nanu DE, Böttger AJ. Phase stabilities of Pd-based alloys for membranes for hydrogen gas separation: a statistical thermodynamics approach. J Alloys Compd 2007;446-447:571–4.
[14] Nanu DE, Böttger AJ. Towards designing stable Pd-based membranes for hydrogen gas separation: a statistical thermodynamics approach. Adv Funct Mater 2008;18(6): 898–906.
[15] Zhang X, Xiong G, Yang W. Hydrogen separation from the mixtures in a thin Pd–Cu alloy membrane reactor. Stud Surf Sci Catal 2007;167:219–24.
[16] Han J, Kim I-S, Choi K.- S. High purity hydrogen generator for on-site hydrogen production. Int J Hydrogen Energy 2002;27: 1043.
[17] Gao HY, Lin YS, Li YD. Chemical stability and its improvement of palladium-based metallic membranes. Ind Eng Chem Res 2004;43:6920.
[18] Mendes D, Chibante V, Zheng J-M, Tosti S, Borgognoni F. Enhancing the production of hydrogen via water gas shift reaction using Pd-based membrane reactors. Int J Hydrogen Energy; 2010.
[19] Iulianelli A, Longo T, Basile A. Methanol steam reforming reaction in a Pd–Ag membrane reactor for CO-free hydrogen production. Int J Hydrogen Energy 2008;33:5583–8.
[20] Basile A, Tereschenko GF, Orekhova NV, Ermilova MM, Gallucci F, Lulianelli A. An experimental investigation on methanol steam reforming with oxygen addition in a flat Pd–Ag membrane reactor. Int J Hydrogen Energy 2006;31: 1615–22.
[21] Grashoff GJ, Pilkington CE, Corti CW. The purification of hydrogen – a review of the technology emphasizing the current status of palladium membrane diffusion. Platinum Met Rev 2009;27(4):157–69.
[22] She Y, Ma YH, Rei MH. Defect-free palladium membranes on porous stainless-steel support. AIChE J 1998;44(2):310–22.
[23] Lewis FA. The palladium hydrogen system: structures near phase transition and critical points. Int J Hydrogen Energy 1995;20(7):587–92.
[24] De Ribaupierre Y, Manchester FD. Experimental study of the critical-point behaviour of the hydrogen in palladium system: I. lattice gas aspects. J Phys C: Solid State Phys 1974; 7:2126–39.
[25] Gremaud R. Hydrogenography: a thin film optical combinatorial study of hydrogen storage materials. Amsterdam: Vrije Universiteit Amsterdam; 2008.

[26] Feenstra R, Griessen R, De Groot DG. Hydrogen induced lattice expansion and effective H–H interaction in single phase PdH_c. J Phys F; Met Phys 1986;16:1933–52.
[27] Feenstra R, De Groot DG, Rector JH, Salomons E, Griessen R. Gravimetrical determinations of pressure-composition isotherms of thin PdHc films. J Phys F; Met Phys 1986;16: 1953–63.
[28] Slaman M, Dam B, Pasturel M, Borsa DM, Schreuders H, Rector JH, et al. Fiber optic hydrogen detectors containing Mg-based metal hydrides. Sens Actuators B Chem 2007;123 (1):538–45.
[29] Slaman M, Dam B, Schreuders H, Griessen R. Optimization of Mg-based fiber optic hydrogen detectors by alloying the catalyst. Int J Hydrogen Energy 2008;33:1084–9.
[30] Gremaud R, Broedersz CP, Borsa DM, Borgschulte A, Mauron P, Schreuders H, et al. Hydrogenography: an optical combinatorial method to find new light-weight hydrogen-storage materials. Adv Mater 2007;19:2813–7.
[31] Gremaud R, Slaman M, Schreuders H, Dam B, Griessen R. An optical method to determine the thermodynamics of hydrogen absorption and desorption in metals. Appl Phys Lett 2007;91:231916.
[32] Gremaud R, Baldi A, Gonzalez-Silveira M, Dam B, Griessen R. Chemical short-range order and lattice deformations in $Mg_yTi_{1-y}H_x$ thin films probed by hydrogenography. Phys Rev B 2008;77:144204.
[33] Howard BH, Killmeyer RP, Rothenberger KS, Cugini AV, Morreale BD, Enick RM, et al. Hydrogen permeance of palladium-copper alloy membranes over a wide range of temperatures and pressures. J Membr Sci 2004;241:207.
[34] Saha DK, Koga K, Ohshima K. Short-range order in Cu–Pd alloys. J Phys Condens Matter 1992;4:10093.
[35] Kikuchi RA. A theory of cooperative phenomena. Phys Rev 1951;81:988–1003.
[36] Pekelharing MI, Böttger AJ, Steenvoorden MP, Van der Kraan AM, Mittemeijer EJ. Application of the cluster variation method to ordering in an interstitial solid solution: calculation of the e-Fe_2N_{1-z}/g′-Fe_4N_{1-x} equilibrium. Philos Mag A 2003;83(15):1775–96.
[37] Sakamoto Y, Ishimaru N, Mukai Y. Thermodynamics of solution of hydrogen in Pd–Cu and Pd–Cu–Au solid solution alloys. Ber Bunsenges Phys Chem 1991;95:680–9.
[38] Shang S, Böttger A. A combined cluster variation method and ab initio approach to the y-Fe[N]/y′-Fe_4N_{1-x} phase equilibrium. Acta Mater 2005;53:255–64.
[39] Burch R, Buss RG. Absorption of hydrogen by palladium–copper alloys. Part 1.—experimental measurements. J Chem Soc Faraday Trans 1975;71(1):913–21.
[40] Schwarz RB, Khachaturyan AG. Thermodynamics of open two-phase systems with coherent interfaces: application to metal–hydrogen systems. Acta Mater 2006;54(2):313–23.
[41] Flanagan TB, Luo S, Clewley D. Calorimetric enthalpies for the reaction of H_2 with Pd–Cu alloys at 303 K. J Alloys Comp 2003;356-357(11):13–6.
[42] Hoang HT, Tong HD, Gielens FC, Jansen HV, Elwenspoek MC. Fabrication and characterisation of dual sputtered Pd–Cu alloy films for hydrogen separation membranes. Mater Lett 2004;58:525–8.
[43] Pundt A, Kirchheim R. Hydrogen in metals: microstructural aspects. Annu Rev Mater Sci 2006;36:555–608.
[44] Schwarz RB, Khachaturyan AG. On the thermodynamics of open two-phase systems with coherent interfaces: application to metal-hydrogen systems. Phys Rev Lett 1995;74:2523.
[45] Wagner H, Horner H. Elastic interaction and the phase transition in coherent metal-hydrogen systems. Adv Phys 1974;23(4):587–637.
[46] Pundt A, Nikitin E, Kirchheim R, Pekarski P. Adhesion energy between metal films and polymers obtained by studying buckling induced by hydrogen. Acta Mater 2004;52:1579.
[47] Fisher D, Chisdes DM, Flanagan TB. Solution of hydrogen in palladium/copper alloys. J Solid State Chem 1977;20: 149–58.